Because the dTip60 complex acetylated nucleosomal phospho-H2Av in vitro, we tested dependence of H2Av acetylation on dTip60 complex components in vivo. We probed chromatin extracts from γ-irradiated double-stranded RNA (dsRNA)–treated S2 cells as well as *dMrg15* mutant embryos with antibodies against H2A(acK5), which recognized H2Av(acK5) (Fig. 3C). We detected transient acetylation of a protein band that exhibits the migratory properties of phospho-H2Av (Fig. 4D). This acetylation was most prominent 15 min after γ irradiation and was not detected in extracts of cells lacking dTip60 or dMrg15. Similar observations were made by immunolabeling *dMrg15* mutant embryos (Fig. 4E and fig. S9). We conclude that the dTip60 complex acetylates nucleosomal phospho-H2Av at Lys^5 in a DSB-dependent manner.

The *Drosophila* dTip60 complex is structurally homologous to its human counterpart (Fig. 1 and table S3) (*17*, *22*, *23*). Both complexes share factors that are linked to cancer, transcription, and DNA repair, including Pontin, Reptin, Mrg15, Tra1, E(Pc), Gas41, and Tip60. We also identified the histone variant H2Av within the *Drosophila* dTip60 complex. The human Tip60 complex is essential for DSB repair and regulation of apoptosis, two processes that have been linked to histone H2Av in flies (*15*, *17*). Also the yeast NuA4 complex appears to accumulate at DSBs (*24*).

We demonstrated that the *Drosophila* dTip60 complex acetylates nucleosomal phospho-H2Av and exchanges it with an unmodified H2Av (Figs. 2 and 3 and figs. S4 to S6). The histone-exchange reaction catalyzed by the ATPase Domino is enhanced by dTip60-mediated acetylation of nucleosomal phospho-H2Av. It appears likely that phospho-H2Av recruits the dTip60 complex to DSBs to facilitate chromatin remodeling during DNA repair. In yeast, the DNA damage–dependent H2A kinase Mec1 genetically interacts with subunits of the NuA4 complex (*21*, *25*), and cells missing NuA4 subunits are sensitive to DSB-inducing agents (*25*, *26*). The physiological roles of the dTip60-mediated phospho-H2Av removal at sites of DSBs could not be clearly separated from a potential function of this complex in DSB repair because of the intimate temporal link between DSB repair and phospho-H2Av clearance (*20*). However, the overexpression of phospho-H2Av did not induce G2/M arrest or affect DSB-dependent G2/M arrest (fig. S10) (*14*, *21*), suggesting that this signal is not sufficient for damage checkpoint control.

The loss of human Tip60 leads to the accumulation of DSBs and is linked to a growing number of cancer types (*26*, *27*). The histone variant H2A.X is essential for genomic stability and a candidate tumor suppressor (*13*, *28*, *29*). Thus, our findings help to understand the functional link between DNA damage–dependent H2A.X phosphorylation and the role of Tip60-type complexes during DSB repair in chromatin.

References and Notes

1. O. Fernandez-Capetillo, A. Celeste, A. Nussenzweig, *Cell Cycle* **2**, 426 (2003).
2. C. Bernstein, H. Bernstein, C. M. Payne, H. Garewal, *Mutat. Res.* **511**, 145 (2002).
3. G. Langst, P. B. Becker, *Biochim. Biophys. Acta* **1677**, 58 (2004).
4. A. Lusser, J. T. Kadonaga, *Bioessays* **25**, 1192 (2003).
5. T. Jenuwein, C. D. Allis, *Science* **293**, 1074 (2001).
6. Y. Wang *et al.*, *Novartis Found. Symp.* **259**, 3 (2004).
7. H. S. Malik, S. Henikoff, *Nat. Struct. Biol.* **10**, 882 (2003).
8. K. Ahmad, S. Henikoff, *Mol. Cell* **9**, 1191 (2002).
9. G. Mizuguchi *et al.*, *Science* **303**, 343 (2004); published online 26 November 2003 (10.1126/science.1090701).
10. M. S. Kobor *et al.*, *PLoS Biol.* **2**, E131 (2004).
11. N. J. Krogan *et al.*, *Mol. Cell* **12**, 1565 (2003).
12. C. Redon *et al.*, *Curr. Opin. Genet. Dev.* **12**, 162 (2002).
13. H. Scherthan, *Cytogenet. Genome Res.* **103**, 235 (2003).
14. C. Redon *et al.*, *EMBO Rep.* **4**, 678 (2003).
15. J. P. Madigan, H. L. Chotkowski, R. L. Glaser, *Nucleic Acids Res.* **30**, 3698 (2002).
16. S. Allard, J. Y. Masson, J. Cote, *Biochim. Biophys. Acta* **1677**, 158 (2004).
17. T. Ikura *et al.*, *Cell* **102**, 463 (2000).
18. Materials and methods are available as supporting material on *Science* Online.
19. T. Kusch, S. Guelman, S. M. Abmayr, J. L. Workman, *Mol. Cell. Biol.* **23**, 3305 (2003).
20. T. Kusch et al., unpublished data.
21. J. A. Downs, N. F. Lowndes, S. P. Jackson, *Nature* **408**, 1001 (2000).
22. Y. Cai *et al.*, *J. Biol. Chem.* **278**, 42733 (2003).
23. Y. Doyon, W. Selleck, W. S. Lane, S. Tan, J. Cote, *Mol. Cell. Biol.* **24**, 1884 (2004).
24. A. W. Bird *et al.*, *Nature* **419**, 411 (2002).
25. J. S. Choy, S. J. Kron, *Mol. Cell Biol.* **23**, 8215 (2002).
26. Y. Doyon, J. Cote, *Curr. Opin. Genet. Dev.* **14**, 147 (2004).
27. K. Halkidou *et al.*, *Oncogene* **22**, 2466 (2003).
28. N. Motoyama, K. Naka, *Curr. Opin. Genet. Dev.* **14**, 11 (2004).
29. O. A. Sedelnikova, D. R. Pilch, C. Redon, W. M. Bonner, *Cancer Biol. Ther.* **2**, 233 (2003).

30. We thank the Bloomington Stock Center and C. Wu, J. Kadonaga, M.-L. Ruhf, and M. Meister for providing reagents. We are indebted to the Stowers core facilities for their support. Special thanks to N. Bae, K. Lee, and K. Trujillo for insightful comments on the manuscript.

Supporting Online Material

www.sciencemag.org/cgi/content/full/1103455/DC1
Materials and Methods
Figs. S1, S2, S4 to S10
Table S3
References and Notes

30 July 2004; accepted 26 October 2004
Published online 4 November 2004;
10.1126/science.1103455
Include this information when citing this paper.

Mammalian Tissue Oxygen Levels Modulate Iron-Regulatory Protein Activities in Vivo

Esther G. Meyron-Holtz, Manik C. Ghosh, Tracey A. Rouault*

The iron-regulatory proteins (IRPs) posttranscriptionally regulate expression of transferrin receptor, ferritin, and other iron metabolism proteins. Although both IRPs can regulate expression of the same target genes, $IRP2^{-/-}$ mice significantly misregulate iron metabolism and develop neurodegeneration, whereas $IRP1^{-/-}$ mice are spared. We found that $IRP2^{-/-}$ cells misregulated iron metabolism when cultured in 3 to 6% oxygen, which is comparable to physiological tissue concentrations, but not in 21% oxygen, a concentration that activated IRP1 and allowed it to substitute for IRP2. Thus, IRP2 dominates regulation of mammalian iron homeostasis because it alone registers iron concentrations and modulates its RNA-binding activity at physiological oxygen tensions.

Iron-regulatory proteins 1 and 2 (IRP1 and IRP2) bind with high affinity to RNA motifs known as iron-responsive elements (IREs) in numerous transcripts related to iron homeostasis. In ferritin H and L chains (H, heart; L, liver), IRP binding near the 5′ end of the mRNA inhibits translation. In contrast, binding of IRPs to IREs in the 3′ portion of the transferrin receptor 1 (TfR1) mRNA stabilizes TfR transcripts (*1*–*3*). Although the genes encoding IRP1 and IRP2 are highly homologous, they sense cytosolic iron levels by different mechanisms. IRP1 is a bifunctional protein; in iron-replete cells, IRP1 contains a cubane [4Fe-4S] cluster and functions as a cytosolic aconitase, interconverting citrate and isocitrate, whereas when the Fe-S cluster is absent, IRP1 apoprotein binds IREs with high affinity (*4*). Unlike IRP1, IRP2 undergoes iron-dependent degradation in iron-replete cells (*5*, *6*). Thus, neither IRP binds to IREs when cells are iron-replete, and ferritin expression increases accordingly, while TfR expression decreases.

In cell lines derived from a wide variety of tissues, IRP1 generally appears to be the major contributor to total iron-regulatory activity (*1*–*3*). In primary cultures of wild-type

Cell Biology and Metabolism Branch, National Institute of Child Health and Human Development, Bethesda, MD 20892, USA.

*To whom correspondence should be addressed. E-mail: trou@helix.nih.gov

(WT) mouse embryonic fibroblasts, IRE-binding activity of IRP1 increased markedly in iron-depleted cells and greatly exceeded that of IRP2 under both iron-replete and iron-depleted conditions (Fig. 1A). In addition, increased IRE-binding activity of IRP1 correlated with a marked decrease in cytosolic aconitase activity (Fig. 1B).

Despite the ability of IRP1 to significantly modulate its IRE-binding activity in cell culture according to iron status, and its ability to regulate expression of target transcripts (*7*, *8*), animals in which IRP1 is genetically ablated display normal regulation of iron metabolism in most tissues (*9*). In contrast, animals that lack IRP2 express abnormally high amounts of ferritin and low amounts of TfR in multiple tissues, and they develop progressive adult-onset neurodegeneration (*10*). In liver lysates from iron-deficient WT animals, the IRE-binding activity of IRP2 increased in response to iron deficiency, whereas the IRE-binding activity and aconitase activity of IRP1 remained constant (Fig. 1, C and D) (*9*).

To understand why the regulatory activities of IRP1 and IRP2 differed in animal tissues compared to cell lines, we analyzed primary cultures of macrophages and lymphocytes from WT, IRP1$^{-/-}$, and IRP2$^{-/-}$ animals. In both cell types, IRP1 appeared to be the predominant IRE-binding protein when cells were cultured in atmospheric oxygen (21% O_2). Because mammalian tissue oxygen concentrations are closer to 3 to 6% than 21% (*11*–*14*), and because IRP activities can be affected by oxygen (*15*), these experiments were carried out at oxygen concentrations ranging from 3 to 21% to evaluate how IRP activities vary accordingly. In macrophages, the change in oxygen concentration from 3 to 21% led to a dramatic switch in the proportion of IRE-binding activity contributed by each IRP. IRP2 was the predominant source of IRE-binding activity at 3% O_2, whereas IRP1 became the major source of IRE-binding activity at 21% O_2. As IRP1 activity increased at 21% O_2, IRP2 levels decreased. In addition, at 3% O_2, IRP1 lost most of its ability to respond to changes in iron status (Fig. 2A and fig. S1). Thus, the relative importance of each IRP in the regulation of iron metabolism varied greatly with changes in oxygen concentration.

In spleen-derived lymphocytes, IRE binding activity of IRP1 also increased markedly as the oxygen concentration rose from 3 to 21% (Fig. 2C). IRP2 levels were highly regulated by iron at all oxygen concentrations examined, although IRP2 protein levels decreased gradually as the oxygen concentration increased (Fig. 2D). Thus, oxygen exposure is a critical variable that determines the potential regulatory activity of IRP1 and IRP2 and their relative importance in both macrophages and lymphocytes.

To evaluate the effect of oxygen-dependent changes of IRP activity on regulated targets, we compared ferritin and TfR expression levels in WT, IRP1$^{-/-}$, and IRP2$^{-/-}$ primary cell cultures grown in 21 or 3 to 6% O_2 concentrations. WT macrophages decreased ferritin and increased TfR expression in response to iron deficiency at both low and high oxygen concentrations (Fig. 3, A and B). In contrast, iron-deficient macrophages from IRP2$^{-/-}$ animals could not repress ferritin or

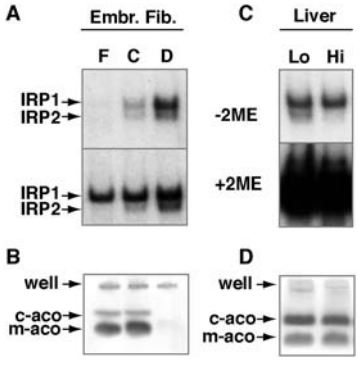

Fig. 1. IRP1 is an effective iron sensor in cultured mouse embryonic fibroblasts, but not in mouse liver. (**A**) Embryonic fibroblasts grown for 16 hours in 21% O_2 in unsupplemented medium (lane C), medium supplemented with 300 μM ferric ammonium citrate (FAC) (lane F), or 100 μM of the iron chelator deferoxamine mesilate (Dfo) (lane D) show increased IRE-binding activity of IRPs in a gel-shift assay in iron-depleted cells. IRP1 can be recruited from its non–IRE-binding form to bind IREs by addition of 2% β-mercaptoethanol (+2ME), which indirectly assesses total IRP1 levels. (**B**) IRP1 from iron-replete cells is an active aconitase (lanes F and C), but IRP1 in iron-depleted cells loses aconitase activity as IRP1 switches to the IRE-binding form (lane D). The mitochondrial aconitase (m-aco) and cytosolic aconitase (c-aco) bands were identified as described (*9*). (**C**) Liver lysates from WT animals on low- or high-iron diets show that IRE-binding activity of IRP2 is regulated according to iron status, whereas IRE-binding activity of IRP1 does not change. Most IRP1 is in a non–IRE-binding form that can be recruited in vitro by +2ME. (**D**) Cytosolic aconitase activities are equal in iron-deficient and iron-replete animals.

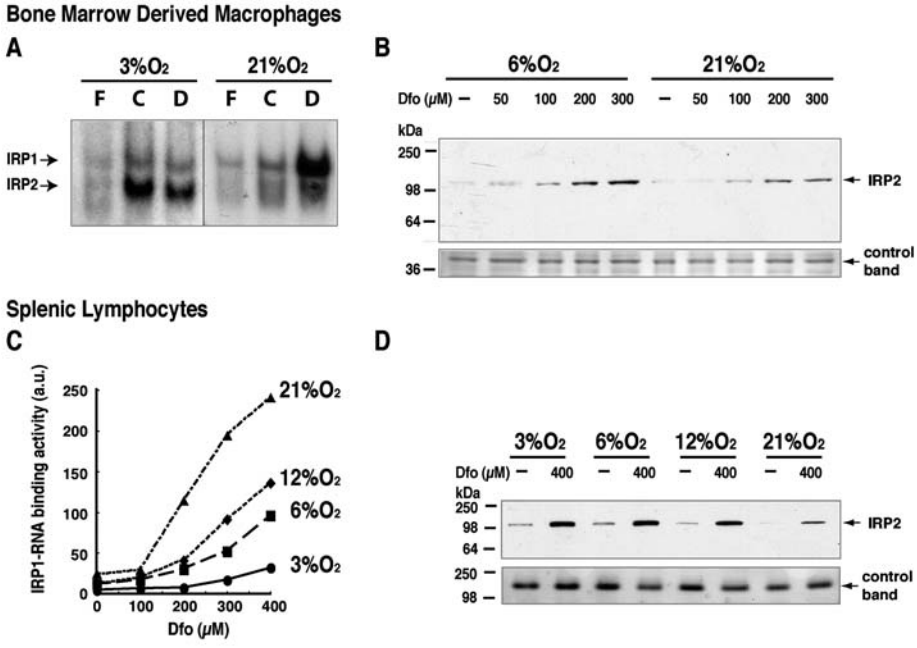

Fig. 2. IRP2 is an effective iron sensor in macrophages and lymphocytes grown at oxygen concentrations ranging from 3 to 21%, whereas IRP1 is a poor sensor at low oxygen concentrations. (**A**) The ratio of IRE-binding activities of IRP1 and IRP2 in macrophages, determined by gel retardation assay, shifts markedly when oxygen concentrations change. After 6 days of growth at 3% O_2, macrophages were exposed for 48 hours to either 3 or 21% O_2 and to iron treatments as described in Fig. 1A. (**B**) IRP2 levels are highly regulated in immunoblot assays of primary WT macrophages at both 6 and 21% O_2 concentrations. After cells were incubated for 6 days at 6% O_2, they were exposed for 48 hours to either 6 or 21% O_2 and treated with a constant amount of 100 μM FAC and increasing amounts of Dfo. To verify even protein loading, we stained immunoblot membranes with PonceauS, and a typical band from this gel is shown. (**C**) IRP1 is a good iron sensor at 21% O_2, but its range of regulation at 3 and 6% O_2 is much lower in lymphocytes. Primary splenic lymphocytes were isolated from WT animals and immediately incubated at 3, 6, 12, and 21% O_2 concentrations for 24 hours in the constant presence of 200 μM FAC and increasing amounts of Dfo. Gel-shift assays were performed to assess IRE-binding activities (fig. S1). IRP1-binding activity was quantified on a Typhoon 9200 Imager (Molecular Dynamics) with Image Quant software. (**D**) IRP2 levels are highly regulated in lymphocytes at multiple oxygen concentrations. Western blots of IRP2 from splenic lymphocytes that were incubated for 72 hours in the constant presence of 200 μM FAC and no Dfo or 400 μM Dfo were probed with antibody to IRP2 as described (*9*). Loading control is the same as in (**B**).

increase TfR expression when grown at 3% O_2. However, at 21% O_2, iron-deficient IRP2$^{-/-}$ macrophages almost fully regulated ferritin and TfR expression, suggesting that the regulatory activity of IRP1 at 21% O_2 allowed IRP1 to substitute for IRP2 in regulation of IRP targets.

Increased ferritin and decreased TfR levels were observed in IRP2$^{-/-}$ macrophage immunoblots grown in 3% O_2 (Fig. 3, A and B) and were attributable to changes in the biosynthetic rates of ferritin and TfR grown at low oxygen concentrations (Fig. 3C). The observation that ferritin and TfR regulation were normal in IRP1$^{-/-}$ macrophages maintained at 3% O_2 implied that IRP2 provided almost all of the regulatory activity in macrophages with minimal contribution from IRP1 at these oxygen concentrations. Levels of IRP2 did not change in IRP1$^{-/-}$ macrophages compared to WT at 3% O_2 (Fig. 3D).

Unlike macrophages, which relied almost exclusively on IRP2 for regulation at physiologically relevant oxygen concentrations, lymphocytes appeared to depend on both IRP1 and IRP2 for normal regulation. The ability to regulate ferritin was significantly reduced in IRP2$^{-/-}$ lymphocytes (Fig. 4A). In IRP1$^{-/-}$ lymphocytes grown at 21% O_2, ferritin levels were also significantly elevated compared to levels in WT controls, and in IRP1$^{-/-}$ lymphocytes grown at 6% O_2, ferritin was slightly elevated at the lowest iron concentration points. These results revealed that IRP1 contributes a substantial fraction of IRE-binding activity in lymphocytes, even though it is minimally sensitive to changes in iron status at low oxygen concentrations (Fig. 2C), similar to its previously observed role in brown fat and kidney (*9*). In lymphocytes, IRP2 levels increased in IRP1$^{-/-}$ cells (Fig. 4B), perhaps because loss of IRP1 resulted in a slight increase in ferritin expression (Fig. 4A) that produced a state of subtle functional cytosolic iron deficiency and a concomitant decrease in the rate of iron-dependent IRP2 degradation (*5*, *6*). The increase in IRP2 allowed cells and tissues to partially compensate for loss of IRP1, as was observed in lymphocytes (Fig. 4B) and in tissues of IRP1$^{-/-}$ mice (*9*). Thus, IRP1 contributes significantly to baseline regulation of iron metabolism in some cells, consistent with the increased severity of neurodegeneration in IRP1$^{+/-}$ IRP2$^{-/-}$ animals (*16*), and the embryonic lethality of IRP1$^{-/-}$ IRP2$^{-/-}$ mice (*17*).

IRP1 and IRP2 operate on a continuum in which the partial pressure of oxygen determines relative activity. IRP1 contains an oxidation-sensitive Fe-S cluster that is enzymatically assembled in cells that have sufficient iron and sulfur (*18*, *19*). However, once the Fe-S cluster of IRP1 is assembled, it may remain stable unless it is exposed to oxidants, including oxygen, superoxide, hydrogen peroxide, nitric oxide, and peroxynitrite (*4*, *20*–*23*). At the ambient oxygen concentrations in tissues of healthy animals (*13*–*15*), the Fe-S cluster of IRP1 appears to be stable, and IRP1 is therefore poorly suited to function as an iron sensor (*9*). In contrast, IRP2 has a different mechanism of iron sensing that depends on iron-dependent degradation (*5*, *6*, *24*–*27*). Iron-dependent turnover is intact at physiologically relevant oxygen concentrations, which enables IRP2 to dominate normal regulation of iron homeostasis in mammals.

IRP1 plays a minor role in the regulation of iron metabolism by contributing a fraction of

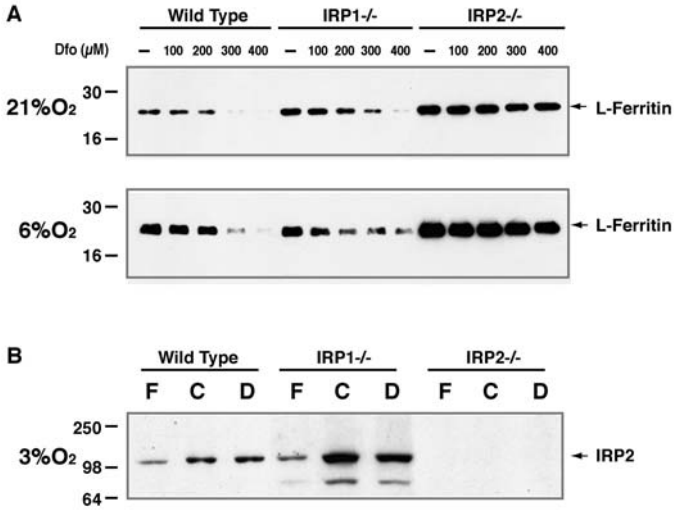

Fig. 4. Misregulation of ferritin occurs in IRP2$^{-/-}$ lymphocytes and to a lesser extent in IRP1$^{-/-}$ lymphocytes, where IRP2 levels increase in compensation for loss of IRP1. (**A**) Lymphocytes were harvested from animals of the different genotypes and grown for 24 hours in 21 or 6% O_2 in the constant presence of 200 μM FAC and various amounts of Dfo. (**B**) In immunoblots on lysates from WT, IRP1$^{-/-}$, and IRP2$^{-/-}$ lymphocytes, IRP2 levels increase substantially in IRP1$^{-/-}$ lymphocytes compared to WT levels. Lymphocytes were grown at 3% O_2 and treated with FAC and Dfo as described in Fig. 3A. Controls for (A) and (B) are given in fig. S3.

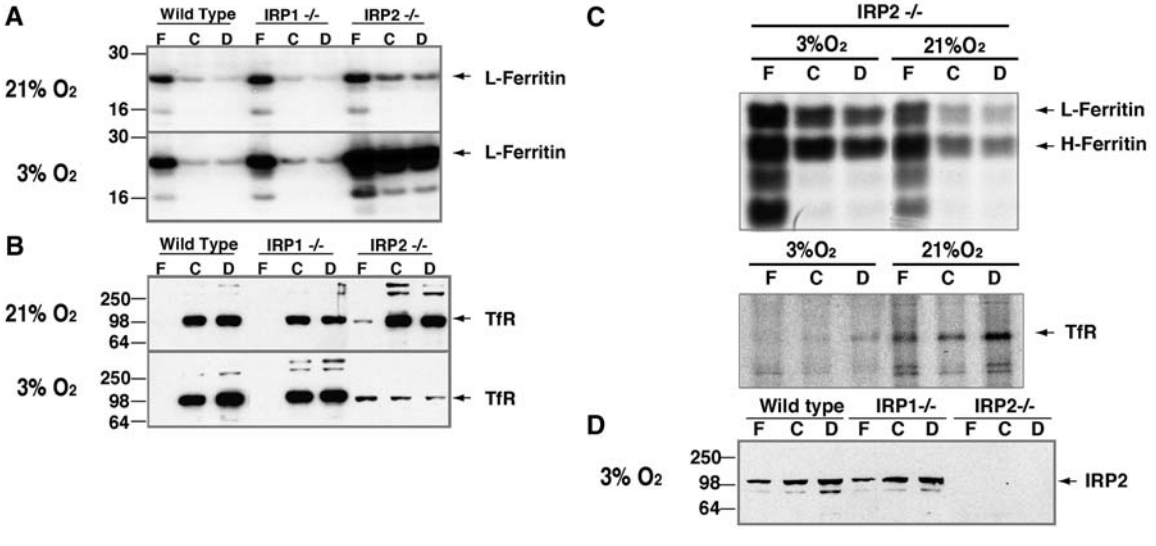

Fig. 3. Misregulation of ferritin and TfR occurs in IRP2$^{-/-}$ macrophages grown at 3% O_2 but not in IRP1$^{-/-}$ macrophages. (**A**) Macrophages were grown for 8 days at either 21 or 3% O_2 and, for the last 48 hours, in either unsupplemented medium (lane C), medium supplemented with 300 μM FAC (lane F), or 100 μM Dfo (lane D). Ferritin levels were detected by immunoblot as described (*30*). (**B**) Levels of TfR were detected by immunoblot in macrophages treated as in (A). (**C**) Ferritin and TfR biosynthesis were assessed by metabolic labeling and immunoprecipitation of ferritin and TfR in macrophages grown at 3% O_2 and treated with FAC and Dfo as described in (A). (**D**) IRP2 levels were assessed by immunoblot in macrophages grown at 3% O_2 and treated with FAC and Dfo as described in (A). Controls for (A), (B), and (D) are given in fig. S2.

baseline IRE-binding activity in tissues. However, the observation that IRE-binding activity can be recruited by oxidative disassembly of its Fe-S cluster means that in some pathological situations, including those in which inflammation results in release of reactive oxygen species, the vast reservoir of IRP1 in the aconitase form (Fig. 1C) may be converted to the IRE-binding form (*20*, *21*). This can lead to inappropriate repression of ferritin synthesis, increased TfR expression, and cellular iron toxicity. Increased iron content coupled with decreased ferritin has been observed in degenerating regions of the brain in Parkinson's disease (*28*). Thus, pathologic activation of IRP1 by reactive oxygen species may play an important role in some disease processes.

Our findings provide genetic evidence that in mammals, the tissue oxygen concentrations are a critical variable in regulating genes that are important in iron metabolism. Results obtained from tissue culture cells grown in room air may lead to conclusions that are not relevant to normal physiology. Iron- and oxygen-based chemistries affect many cellular processes, including mitochondrial function, DNA replication, and the response to hypoxia (*29*). Our work demonstrates that the IRP-regulatory system has evolved to tightly regulate iron metabolism at oxygen concentrations that exist in normal mammalian tissues. Even though the two IRPs are highly homologous (*1*), their activities are only partially redundant, and they occupy different regulatory niches. In normal physiology, tissue oxygen tension determines the contribution of each IRP to the regulation of iron homeostasis.

References and Notes

1. T. Rouault, R. Klausner, *Curr. Top. Cell. Regul.* **35**, 1 (1997).
2. B. D. Schneider, E. A. Leibold, *Curr. Opin. Clin. Nutr. Metab. Care* **3**, 267 (2000).
3. M. W. Hentze, M. U. Muckenthaler, N. C. Andrews, *Cell* **117**, 285 (2004).
4. H. Beinert, M. C. Kennedy, D. C. Stout, *Chem. Rev.* **96**, 2335 (1996).
5. B. Guo, J. D. Phillips, Y. Yu, E. A. Leibold, *J. Biol. Chem.* **270**, 21645 (1995).
6. K. Iwai *et al.*, *Proc. Natl. Acad. Sci. U.S.A.* **95**, 4924 (1998).
7. P. A. DeRusso *et al.*, *J. Biol. Chem.* **270**, 15451 (1995).
8. J. Wang, K. Pantopoulos, *Mol. Cell. Biol.* **22**, 4638 (2002).
9. E. G. Meyron-Holtz *et al.*, *EMBO J.* **23**, 386 (2004).
10. T. LaVaute *et al.*, *Nat. Genet.* **27**, 209 (2001).
11. Q. Chen *et al.*, *Proc. Natl. Acad. Sci. U.S.A.* **92**, 4337 (1995).
12. M. Erecinska, I. A. Silver, *Respir. Physiol.* **128**, 263 (2001).
13. P. O. Carlsson, F. Palm, A. Andersson, P. Liss, *Diabetes* **50**, 489 (2001).
14. L. Studer *et al.*, *J. Neurosci.* **20**, 7377 (2000).
15. E. S. Hanson, M. L. Rawlins, E. A. Leibold, *J. Biol. Chem.* **278**, 40337 (2003).
16. S. R. Smith *et al.*, *Ann. N. Y. Acad. Sci.* **1012**, 65 (2004).
17. S. R. Smith, T. A. Rouault, unpublished observations.
18. W. H. Tong, T. A. Rouault, *EMBO J.* **19**, 5692 (2000).
19. W. H. Tong *et al.*, *Proc. Natl. Acad. Sci. U.S.A.* **100**, 9762 (2003).
20. K. Pantopoulos *et al.*, *J. Biol. Chem.* **272**, 9802 (1997).
21. E. S. Hanson, E. A. Leibold, *Gene Expr.* **7**, 367 (1999).
22. C. Bouton, J. C. Drapier, *Sci. STKE* **2003**, pe17 (2003).
23. G. Cairo *et al.*, *Biochemistry* **41**, 7435 (2002).
24. K. Yamanaka *et al.*, *Nat. Cell Biol.* **5**, 336 (2003).
25. J. Wang *et al.*, *Mol. Cell. Biol.* **24**, 954 (2004).
26. L. S. Goessling, D. P. Mascotti, R. E. Thach, *J. Biol. Chem.* **273**, 12555 (1998).
27. E. Bourdon *et al.*, *Blood Cells Mol. Dis.* **31**, 247 (2003).
28. D. T. Dexter *et al.*, *Ann. Neurol.* **32** (suppl.), S94 (1992).
29. C. J. Schofield, P. J. Ratcliffe, *Nat. Rev. Mol. Cell Biol.* **5**, 343 (2004).
30. Materials and methods are available as supporting material on *Science* Online.

31. This work was supported by the intramural program of the National Institute of Child Health and Human Development and in part by the Lookout Foundation.

Supporting Online Material

www.sciencemag.org/cgi/content/full/306/5704/2087/DC1
Materials and Methods
Figs. S1 to S3
References

9 August 2004; accepted 22 October 2004
10.1126/science.1103786

Hepcidin Regulates Cellular Iron Efflux by Binding to Ferroportin and Inducing Its Internalization

Elizabeta Nemeth,[1] Marie S. Tuttle,[2] Julie Powelson,[2] Michael B. Vaughn,[2] Adriana Donovan,[3] Diane McVey Ward,[2] Tomas Ganz,[1]* Jerry Kaplan[2]*

Hepcidin is a peptide hormone secreted by the liver in response to iron loading and inflammation. Decreased hepcidin leads to tissue iron overload, whereas hepcidin overproduction leads to hypoferremia and the anemia of inflammation. Ferroportin is an iron exporter present on the surface of absorptive enterocytes, macrophages, hepatocytes, and placental cells. Here we report that hepcidin bound to ferroportin in tissue culture cells. After binding, ferroportin was internalized and degraded, leading to decreased export of cellular iron. The posttranslational regulation of ferroportin by hepcidin may thus complete a homeostatic loop: Iron regulates the secretion of hepcidin, which in turn controls the concentration of ferroportin on the cell surface.

The liver-produced hormone hepcidin controls plasma iron levels by regulating the absorption of dietary iron from the intestine, the release of recycled hemoglobin iron by macrophages, and the movement of stored iron from hepatocytes [for a review, see (*1*, *2*)]. During pregnancy, fetal hepcidin controls the transfer of maternal iron across the placenta to the fetus. In turn, hepcidin levels are homeostatically regulated by hepatic iron and by the need for erythropoiesis as sensed by liver oxygenation. Hepcidin is also induced during inflammation, in which hepcidin's effect on iron transport causes the characteristic decrease in blood iron (hypoferremia of inflammation). The hypoferremia is thought to increase host resistance to microbial infection but also leads to the anemia of inflammation (often referred to as the anemia of chronic disease).

Ferroportin (Fpn) is an iron exporter on the surface of absorptive intestinal enterocytes, macrophages, hepatocytes, and placental cells, all of which release iron into plasma (*3*–*5*). To determine whether hepcidin interacts with Fpn, we generated a stable cell line (HEK293-Fpn) expressing mouse Fpn with a C-terminal green fluorescent protein (GFP) under the control of the ecdysone-inducible promoter. In the absence of the inducer ponasterone, there was no detectable synthesis of Fpn-GFP. Within 24 hours of ponasterone addition, there was abundant GFP fluorescence outlining the surface of cells (fig. S1). To determine whether Fpn-GFP was functional, we examined the effect of ferroportin induction on cellular iron levels, as measured by the accumulation of ferritin, the cytosolic iron storage protein. Incubation of cells with ferric ammonium citrate (FAC) alone resulted in a large increase in ferritin levels. FAC loading with simultaneous induction of Fpn-GFP prevented ferritin accumulation (Fig. 1A). Similar results were obtained when diferric transferrin was used as an iron source and levels of IRP2, inversely regulated by cytosolic iron (*6*, *7*), were measured as an indicator of cellular iron levels (fig. S2). Induction of Fpn-GFP resulted in an increase of IRP2 levels when compared to uninduced cells, indicating that cytosolic iron levels decreased after the induction of Fpn-GFP. To show that reduced cytosolic iron levels re-

[1]Department of Medicine, David Geffen School of Medicine, University of California, Los Angeles, CA, USA. [2]Department of Pathology, School of Medicine, University of Utah, Salt Lake City, UT, USA. [3]Department of Hematology, Children's Hospital, Boston, MA, USA.

*To whom correspondence should be addressed. E-mail: TGanz@mednet.ucla.edu (T.G.); jerry.kaplan@path.utah.edu (J.K.)